

RESEARCH

Open Access



BCR::ABL1 expression in chronic myeloid leukemia cells in low oxygen is regulated by glutamine via CD36-mediated fatty acid uptake

Caterina Mancini², Giulio Menegazzi¹, Silvia Peppicelli¹, Giampaolo Versenti¹, Daniele Guasti², Giuseppe Pieraccini³, Elisabetta Rovida¹, Matteo Lulli¹, Laura Papucci¹, Persio Dello Sbarba^{1*} and Alessio Biagioni^{1*}

Abstract

Background Chronic myeloid leukemia (CML) is influenced by microenvironmental nutrients, glucose (Glc), and glutamine (Gln) which regulate cell proliferation, viability, and the expression of the driver oncoprotein (BCR::ABL1).

Results Our study revealed that Glc, while partially supporting alone cell growth in normoxia, is essential in low oxygen conditions, whereas Gln is ineffective. Under low oxygen, Gln reduced oxidative respiratory activity while enhancing glycolysis. In these conditions, fatty acid (FA) metabolism becomes crucial, as evidenced by increased lipid droplets (LD) accumulation when Glc was absent. Gln, in particular, drives CD36-mediated FA uptake, suppressing the BCR::ABL1 oncoprotein and facilitating cell survival. By co-culturing leukemia cells with adipocytes, one of the main bone marrow (BM) cell components, we observed an enhanced FA release, suggesting a link between FA, microenvironmental BM cells, and the maintenance of leukemic stem cells (LSC).

Methods K562 and KCL22 cell lines were subjected to Glc and/or Gln deprivation under hypoxic conditions (96 h at 0.1% O₂). Metabolic profiling was conducted through the Seahorse XFe96 analyzer, and the contribution of L-Glutamine-¹³C₅ to FA *de novo* synthesis was determined via GC/MS. Intracellular neutral LD were measured using BODIPY 493/503 in confocal microscopy and flow cytometry, with their presence and morphology further examined via transmission electron microscopy. BCR::ABL1 as well as several FA-related markers were evaluated via Western Blotting, whilst CD36 was determined through flow cytometry. LC2 assay was used for measuring leukemia stem cell potential by inhibiting FA uptake via the usage of the Sulfo-N-Succinimidyl Oleate, a CD36 inhibitor. qPCR was exploited to detect markers of FA secretion in CML-adipocytes co-culture together with Nile Red staining to assess free FA in the media.

*Correspondence:
Persio Dello Sbarba
persio.dello sbarba@unifi.it
Alessio Biagioni
alessio.biagioni@unifi.it

Full list of author information is available at the end of the article



© The Author(s) 2025. **Open Access** This article is licensed under a Creative Commons Attribution-NonCommercial-NoDerivatives 4.0 International License, which permits any non-commercial use, sharing, distribution and reproduction in any medium or format, as long as you give appropriate credit to the original author(s) and the source, provide a link to the Creative Commons licence, and indicate if you modified the licensed material. You do not have permission under this licence to share adapted material derived from this article or parts of it. The images or other third party material in this article are included in the article's Creative Commons licence, unless indicated otherwise in a credit line to the material. If material is not included in the article's Creative Commons licence and your intended use is not permitted by statutory regulation or exceeds the permitted use, you will need to obtain permission directly from the copyright holder. To view a copy of this licence, visit <http://creativecommons.org/licenses/by-nc-nd/4.0/>.

Conclusions These findings underscore the central role of FA in the regulation of the LSC compartment of CML, highlighting the importance of Gln in facilitating CML cell survival under restrictive metabolic conditions and preparing the cell population for expansion upon the release of these restrictions.

Keywords Chronic myeloid leukemia, Hypoxia, BCR:ABL1, Fatty acids

Backgrounds

Chronic myeloid leukemia (CML) is a myeloproliferative disease triggered by t(9;22) translocation, resulting in the expression of the fusion oncoprotein BCR::ABL1, a constitutively active tyrosine kinase [1]. Despite the efficiency of tyrosine kinase inhibitors (TKi), such as imatinib mesylate (IM), which is capable of targeting the ATP-binding site of BCR::ABL1, thereby inhibiting its enzymatic activity, the therapy does not cure CML. Indeed, the persistence of a subpopulation of TKi-resistant leukemia stem cells (LSC) sustains so-called minimal residual disease (MRD).

The LSC subset sustaining MRD is likely genetically BCR::ABL1-positive, but oncoprotein-negative [2, 3]. LSC, like normal hematopoietic stem cells (HSC), are believed to persist in bone marrow (BM) stem cell niches (SCN), which are physiologically characterized by severe metabolic limitations due to reduced oxygen and nutrient supply. Indeed, HSC are better maintained and enriched in low oxygen conditions than under standard normoxic incubation conditions, whereas non-stem clonogenic hematopoietic progenitor cells are suppressed in low oxygen [4]. This led to the proposal of the “hypoxic” SCN model, a tissue microenvironment in which oxygen tension is physiologically much lower than in other tissue zones, and to set the stage to study molecular mechanisms enabling HSC to reside in and adapt to low oxygen, while maintaining the capacity to cycle and expand [5]. Our laboratory has previously demonstrated that, under very low oxygen tension, while CML cells undergo suppression of the BCR::ABL1 oncoprotein, a BCR::ABL1-independent LSC subset survives and retains the capacity, when transferred to conditions permissive for growth (“normoxia”), to generate a BCR::ABL1-expressing progeny that then undergoes clonal expansion [6]. A crucial point is that LSC adapted to low oxygen levels are resistant to IM and other TKi used for CML treatment, as they lack the molecular target (i.e. BCR::ABL1 oncoprotein).

We also demonstrated that the suppression of BCR::ABL1 oncoprotein is induced by glucose (Glc) shortage in a low oxygen environment, favored by the “Pasteur effect” [7], as well as in normoxic conditions [8]. Based on this evidence, we proposed a model of low-oxygen SCN where BCR::ABL1 oncoprotein-positive or -negative LSC subsets are spatially distributed according to local substrate availability and as a function of their different metabolic profiles [9]: where Glc is available,

BCR::ABL1 expression is fostered and thereby LSC are pushed to undergo clonal expansion, whereas zones characterized by Glc shortage would host slow-cycling/self-renewing LSC adapted to persist independently of BCR::ABL1 signaling, which determines their refractoriness to TKi and sustains the maintenance of TKi-resistant MRD.

Glc and glutamine (Gln) control cell survival, proliferation, and differentiation through highly interconnected bioenergetic pathways [10]. In another study, we recently addressed the role of Gln availability in controlling BCR::ABL1 expression in CML cells incubated under very low oxygen tension, with or without BPTES, the glutaminase inhibitor, demonstrating that under these conditions, Glc consumption is positively regulated by Gln [11]. Indeed, Gln starvation has already been demonstrated to slow down Glc catabolism and weaken cell adaptation to low oxygen [12, 13]. Because Glc shortage does not affect the maintenance of stem cell potential in BCR::ABL1 protein-negative CML cells, the key question is which source of energy these cells rely on.

Under oxygen shortage, cancer cells undergo a deep metabolic switch, stimulating glycolysis and inhibiting mitochondrial metabolism, mainly through the activation of pyruvate dehydrogenase kinase isoenzyme 1, which in turn inhibits the pyruvate dehydrogenase complex, blocking the conversion of pyruvate to acetyl-CoA, thus preventing ATP production via the Tricarboxylic Acid (TCA) cycle [14]. However, the effects of low oxygen tension on lipid metabolism are still debated and require further investigation. Fatty acids (FA) are commonly provided by exogenous uptake or *de novo* synthesis and, once available for cell utilization, are exploited as substrates for oxidation and energy production, membrane synthesis, and production of signaling molecules, or esterified and stored in the form of triacylglycerols (TAG) [15]. FA synthesis is a biological process that is closely related to the TCA cycle and is commonly strongly inhibited under low oxygen conditions. Furthermore, FA synthesis requires a relatively high amount of ATP, which is not abundant when the nutrients are scarce. Therefore, under nutrient shortage conditions, cells seek exogenous FA. Uptake of extracellular FA and TAG synthesis is promoted under low-oxygen conditions by PPAR γ , the gene expression of which is in cancer cells directly activated by HIF-1 [16] and fatty acid-binding protein (FABP) 3, 4, and 7 [17, 18].

In this study, we focused on how the lack of oxygen affects energy metabolism in CML cells and, in particular,

how Glc and Gln availability regulate lipid metabolism and cell energy demand under low oxygen conditions. These metabolic cues were also related to the regulation of BCR::ABL1 protein expression and stem cell potential.

Methods

Cell lines

The K562 (RRID: CVCL_0004) and KCL22 (RRID: CVCL_2091) BCR::ABL1-positive cell lines derived from CML patients in blast crisis were cultured in RPMI 1640 medium supplemented with 10% fetal bovine serum and 2 mM Gln (Euroclone, Milan, Italy) and incubated at 37 °C in 5% CO₂ atmosphere. K562 is a lymphoblastic cell line isolated from the BM of a 53-year-old blast phase CML patient while KCL22, isolated from the pleural effusion of a 32-year-old female CML patient at blast crisis, exhibits a lymphoblast-like morphology; both are characterized by the Philadelphia chromosome. Experiments were performed with cells harvested from exponentially growing maintenance cultures and plated at 3 × 10⁵/mL, to be incubated at 37 °C under “normoxic” conditions (21.0% O₂, atmosphere containing air/5% CO₂) or low-oxygen atmosphere (0.1% O₂, 5% CO₂, and 94.9% N₂) in a gas-tight manipulator/incubator (DG250 Anaerobic Workstation; Don Whitley Scientific; Shipley, Bridgend, UK). Glc or Gln starvation was performed using RPMI 1640 medium without Glc and Gln (Sartorius, Rome, Italy) and singularly adding 2 g/L D-glucose (Thermo Fisher Scientific, Monza, Italy) or 2 mM L-glutamine (Euroclone). Cell viability was measured using trypan blue (Sigma-Aldrich, Milan, Italy) exclusion test.

Seahorse metabolic assays

The respiratory and glycolytic capacities of the CML cells were evaluated using a Seahorse XFe96 Analyzer (Seahorse Bioscience, Billerica, MA, USA). Briefly, 7 × 10⁴ cells/well were seeded in XFe96 microplates pre-coated with poly-D-lysine (Thermo Fisher Scientific). Before analysis, cells were resuspended in Seahorse assay buffer specific for Glycolysis Stress, Mito Stress or Mito Fuel Flex Assays, and the following drugs were added: for Glycolysis Stress Assay, 10 mM glucose, 1 μM oligomycin, and 50 mM 2-deoxy-D-glucose (2-DG); Mito Stress Assay 1 μM oligomycin, 1 μM carbonyl cyanide-4-(trifluoromethoxy)phenylhydrazone (FCCP), 0.5 μM rotenone/antimycin A; Mito Fuel Flex Test, 4 μM Eto-moxir, 3 μM Bis-2-(5-phenylacetamido-1,3,4-thiadiazol-2-yl)ethyl sulfide (BPTES), 2 μM UK5099 (all reagents provided by Agilent, Milan, Italy). The results were normalized with respect to the protein content of the samples as evaluated using the BCA assay. The experiments were performed in five technical replicates and at least three biological replicates. The SeaHorse XF Report Generator automatically calculated the parameters from wave

data that had been exported to Prism, while the fuel oxidation dependency was calculated using the equation

$$\text{Dependency \%} = \left[\frac{\text{Baseline OCR} - \text{Target Inhibitor OCR}}{\text{Baseline OCR} - \text{All inhibitors OCR}} \right] * 100.$$

Transmission electron microscopy

Cells were centrifuged at 1000 rpm for 5 min in 1.5 mL Eppendorf tubes. The resulting cell pellet was fixed in isotonic 4% glutaraldehyde and 1% osmium tetroxide (OsO₄), then dehydrated and embedded in Epon epoxy resin (Fluka, Buchs, Switzerland). Ultrathin sections were stained with 1% samarium triacetate-10% gadolinium triacetate (UAR-EMS stain #22405; Electron Microscopy Sciences, Hatfield, PA, USA), counterstained with lead citrate, and examined under a JEM 1010 transmission electron microscope (Jeol, Tokyo, Japan) equipped with a MegaView III high-resolution digital camera and imaging software (Jeol).

Flow cytometry

Cells were washed once with cold PBS and then stained with fluorochrome-conjugated antibody anti-CD36 (Immunotools, Friesoythe, Germany) for 1 h at 37 °C in the dark or with BODIPY 493/503 (final concentration 5 μM– Thermo Fisher), a dye specifically staining neutral lipids, for 30 min at 37 °C in the dark. The cells were then analyzed using a BD-FACS Canto II flow cytometer, and the data was elaborated using Flowjo Software (RRID: SCR_008520) (BD Biosciences, Milan, Italy).

Nile red staining

Conditioned media were collected by discarding the cell pellet after centrifugation at 300 g for 5 min, and lipids were stained by adding the Nile Red dye (Thermo Fisher) [19], which had been previously dissolved in DMSO (starting concentration 1 mM, final concentration 1 μM), for 30 min at 37 °C in dark. Fluorescence intensity was measured with an ELISA multi-plate reader (Biotek Synergy H1, Agilent) at an excitation wavelength of 515 nm and emission wavelength of 585 nm, and the values were normalized on the basis of viable cell counts following trypan blue staining.

Confocal microscopy

For immunofluorescence confocal microscopy, cells were plated on μ-Slide 8 Well (Ibidi, Rome, Italy), according to routine methods. BODIPY staining was performed as previously described, and the slides were imaged using a Leica SP8 confocal laser scanning microscope equipped for fluorescence measurements (Leica; Milan, Italy). Lipid droplet (LD) quantification was performed using ImageJ software (RRID: SCR_003070) (developed by

Wayne Rasband, National Institutes of Health, Bethesda, MD, USA) as previously reported [20].

Gas chromatography-mass spectrometry

For FA analysis cell extracts were analyzed by gas chromatography-mass spectrometry (GC-MS) using an Agilent 6890 gas chromatograph, equipped with a 7683 Injector and coupled to a 5973 mass spectrometer (Agilent); the capillary column was a Zebron ZB-WAX plus, 25 m x 0.25 mm, 0.25 μ m film thickness (Phenomenex Italia, Bologna, Italy); the oven program was as follows: time 0 min, 100 °C for 2 min, followed by an increase of 15 °C/min up to 175 °C, then an increase of 3 °C/min up to 250 °C, and held for 10 min. A 1 μ L volume was injected in splitless mode (2 min valve off); injector and transfer line temperatures were 250 and 255 °C, respectively. Helium was used as the carrier gas at a constant flow rate of 1 ml/min. The 70 eV EI source was maintained at 230 °C and a quadrupole analyzer at 150 °C. MS data were acquired in scan mode from 50 to 550 m/z (2.9 scan/min rate).

The FA in the sample were analyzed following their conversion to methyl esters (FAME). FAME were prepared by adding BF₃ in methanol (12–14%, w/v) and incubating the samples at 40 °C for 30 min. Water was then added, and the FAME was extracted with hexane and analyzed by GC-MS. Some of the samples were used for the analysis of free FA (FFA). FFA was extracted with hexane, and the organic solvent was dried under a gentle N₂ flow before GC-MS analysis. Another part of the sample was used to determine total FA content. FAME were obtained by esterification and trans-esterification by adding 1 mL of a freshly prepared solution of 2% (v/v) concentrated sulfuric acid in methanol. The samples were left at 70 °C for 3 h; then, 1 mL of water was added, and FAME extracted with 3 x 3 mL of hexane. The organic solvent was then dried under a gentle N₂ flow before GC-MS analysis. Each sample was injected in triplicate, and the intensities of the molecular ions of the methyl esters of palmitic, oleic, and stearic acids were measured along with those of the M + 1 and M + 2 ions in their isotopic profiles. The ratio between these ions was measured for each acid and evaluated to verify whether the M + 1 and/or M + 2 ion intensities were different from those of the control samples.

For lactate analysis cells subjected to 4 days of severe hypoxia (0.1% O₂) were prepared for GC-MS on an Intuvo9000/5977 B MSD (Agilent Technologies, Santa Clara, CA, USA) via selected ion monitoring (SIM) mode MS. Cells were washed twice with 0,9% NaCl at 4 °C and scraped in 400 μ l of cold (-20 °C) 80% methanol in water (containing 1 μ g/mL norvaline as internal standard). Samples were sonicated on ice for 5 s for 3 times with a 5 s interval at 70% amplitude, centrifuged at 14,000 rpm,

4 °C for 10 min, and supernatants were collected and lyophilized. Cell pellets were resuspended in 50 μ l of 200 mM NaOH, denatured at 96 °C for 15 min, centrifuged at 14,000 rpm for 5 min, and used for establishing the protein concentration per sample for final normalization [21].

Western blotting

Cells were lysed in RIPA buffer (Merck Millipore, Milan, Italy) containing PMSF (Sigma-Aldrich), sodium orthovanadate (Sigma-Aldrich), and protease inhibitor cocktail (Calbiochem, San Diego, CA, USA). Lysates were sonicated and centrifuged for 15 min at 14,000 rpm at 4 °C. The protein content of cell lysates was measured using the BCA method. 50 μ g of protein lysate was separated on NuPAGE Tri-Acetate 3–8% precast polyacrylamide gels and subsequently transferred to a PVDF membrane using the iBlot 3 System (all from Thermo Fisher Scientific). After blocking for 1 h with Odyssey blocking buffer (BioClass, Pistoia, Italy), the membrane was incubated overnight at 4 °C with the primary antibodies. The primary antibodies used included anti-vinculin (sc-73614, 1:1000; Santa Cruz Biotechnology), anti-c-Abl (sc-131, 1:1000; Santa Cruz Biotechnology), anti-phospho-CrkL (#3181 1:1000; Cell Signaling), and anti-FASN (#3180, 1:1000; Cell Signaling) (Milan, Italy). The protein bands were analyzed using the Odyssey Infrared Imaging System (Licor Bioscience, Lincoln, NE, USA) and quantified via ImageJ software (RRID: SCR_003070).

Measure of stem/progenitor cell potential

The stem/progenitor cell potential of the cultures was assessed using the Culture Repopulation Ability (CRA) assay, a non-clonogenic assay capable of estimating in vitro the content of a hematopoietic cell population with stem/progenitor cells endowed with BM Repopulation Ability in vivo. Cells rescued from experimental cultures subjected to selective treatment (liquid culture 1, LC1) were transferred to non-selective assay cultures (LC2) where the stem/progenitor cell potential of input cells was actualized and maximally exploited. The measurement of LC2 repopulation via the count of the total number of viable cells provides an estimate of the stem/progenitor cell potential of LC1 cells at the end of incubation therein [11, 22]. In the study reported here, 3 x 10⁵ cells/mL were incubated for 4 days in experimental LC1 incubated in low oxygen, in the absence or presence of Glc and/or Gln, and drug-treated or untreated. At the end of the incubation, LC1 cells were washed free of the drug and transferred (3 x 10⁴ cells/mL) to the growth-permissive assay LC2. The time required for LC1 cells to reach the peak of LC2 repopulation (and, in particular, the presence or absence of a lag phase before

repopulation starts) is a distinctive property of the stem/progenitor cell subset transferred from LC1, whereas the area underlying the LC2 repopulation curve correlates with the level of maintenance of stem/progenitor cell potential in LC1 [23].

Reagents

Sulfo-N-succinimidyl oleate (MedChemExpress, Sollen-tuna, Sweden) was dissolved in DMSO (100 mM) and used at a final concentration of 150 μ M to avoid any possible cytotoxic effects. Etomoxir was dissolved in DMSO (10 mM) and used at a final concentration of 4 μ M (Med-ChemExpress). Bovine Serum Albumin (BSA) and palmitate were provided by Sigma-Aldrich. We aim to specify that we used Palmitate as an exogenous source of FA as it is a single, well-characterized saturated FA, chemically stable and commonly one of the most abundant in mammalian cells, derived from both dietary sources and *de novo* lipogenesis. Moreover, it is also well tolerated by cells at low concentrations and rapidly used for FA oxidation [24].

RNA extraction and quantitative PCR

Total RNA was extracted using Tri Reagent (Sigma-Aldrich) and reverse transcribed (from 500 ng to 1 μ g measured through Thermo Fisher Scientific NanoDropOne) by using the cDNA synthesis kit (BioRad) following the manufacturer's instructions. The expression of selected genes was evaluated via Real-Time RT-PCR (qPCR) with the Sso Advanced Universal Green Mix (Bio-Rad) in the Bio-Rad CFX96 qPCR System (Bio-Rad). The qPCR amplification steps included polymerase activation at 95 °C for 3 min, denaturation at 95 °C for 10 s, and annealing/extension at 60 °C for 30 s (the last two steps repeated for 40 cycles). Melt curve analysis was performed for each qPCR run according to the Bio-Rad CFX96 protocol. Fold changes in gene expression were determined using the comparative Ct method, with GAPDH, BACT, and 18 S rRNA as normalization genes. Primer sequences were provided by IDT (Tema Ricerca, Bologna, Italy).

Co-culture model

HS27A (RRID: CVCL_3719) is a fibroblast cell line derived from healthy BM that retains the capacity to differentiate when subjected to specific stimuli. Here, 4×10^4 cells/well were seeded in a 12-well plate and treated with StemMacs AdipoDiff medium (Miltenyi, Bologna, Italy) for 10 days, replacing the medium with fresh medium every 3 days. Once HS27A cells acquired the mature adipocyte phenotype, they were co-cultured with CML cells (ratio 1:1) in their medium mixed 1:1 with RPMI medium for two days in low oxygen.

Statistics

Data are expressed as the mean \pm SD or \pm SEM, as specified in each figure legend, of the data from at least three independent experiments. All statistical analyses were performed by using GraphPad Prism 10.4.1 (RRID: SCR_002798). For multiple comparisons, we used two-way ANOVA, to assess the effects of different experimental conditions and in particular: when the reference control was Glc (+) Gln (+) as in the left panel of Fig. 1, we applied the Dunnet's multiple comparison test, which allows comparison of multiple conditions to a single control; when comparing all conditions against each other, we used Sidak's multiple comparison test, which is more suitable for multiple comparisons while maintaining statistical power. For LD counting in Fig. 5B, an unpaired two-tailed Student's t-test was used to compare the two experimental groups, assuming equal variance. Statistical significance was set at $p < 0.05$. Significance levels are reported above each histogram.

Results

Effects of glucose and/or glutamine on CML cell survival and proliferation

We first assayed the effects of the absence of Glc or Gln in the culture medium on CML cell proliferation as shown in Fig. 1. The presence of both Glc and Gln (condition Glc+/Gln+) fueled cell proliferation in "normoxic" conditions and only transiently (until days 2–3) in low oxygen conditions. Glc alone (no Gln; Glc+/Gln-) was, on the contrary, incapable (Fig. 1A) or partially capable (Fig. 1B) of supporting cell growth in "normoxia" but fully sustained cell number increase in low oxygen conditions (Fig. 1A, B). Gln alone (no Glc; Glc-/Gln+) was unable to support cell growth under either "normoxia" or low oxygen. In the latter case, the number of viable cells decreased steadily from the beginning of incubation. Indeed, Glc and Gln control cell survival and cycle progression through highly interconnected bioenergetic pathways [25]. While Glc is commonly referred to as the most ready-to-use energy source, especially for tumor cells, Gln plays a major role in low-oxygen tissues, such as the SCN, interfering with Glc catabolism and weakening cell adaptation to hypoxia [12]. In our experimental model, Gln was able to maintain CML cells alive in the absence of Glc only when oxygen supported the oxidative phosphorylation pathway. On the other hand, Glc is necessary and sufficient for cell survival and growth under low-oxygen conditions. The latter finding led to the exclusion of the withdrawal of both Glc and Gln (condition Glc-/Gln-) for further experiments in low oxygen, a combination unable to ensure cell survival in culture. On the other hand, the results obtained allowed a set of four days of incubation in the presence of Glc as a time

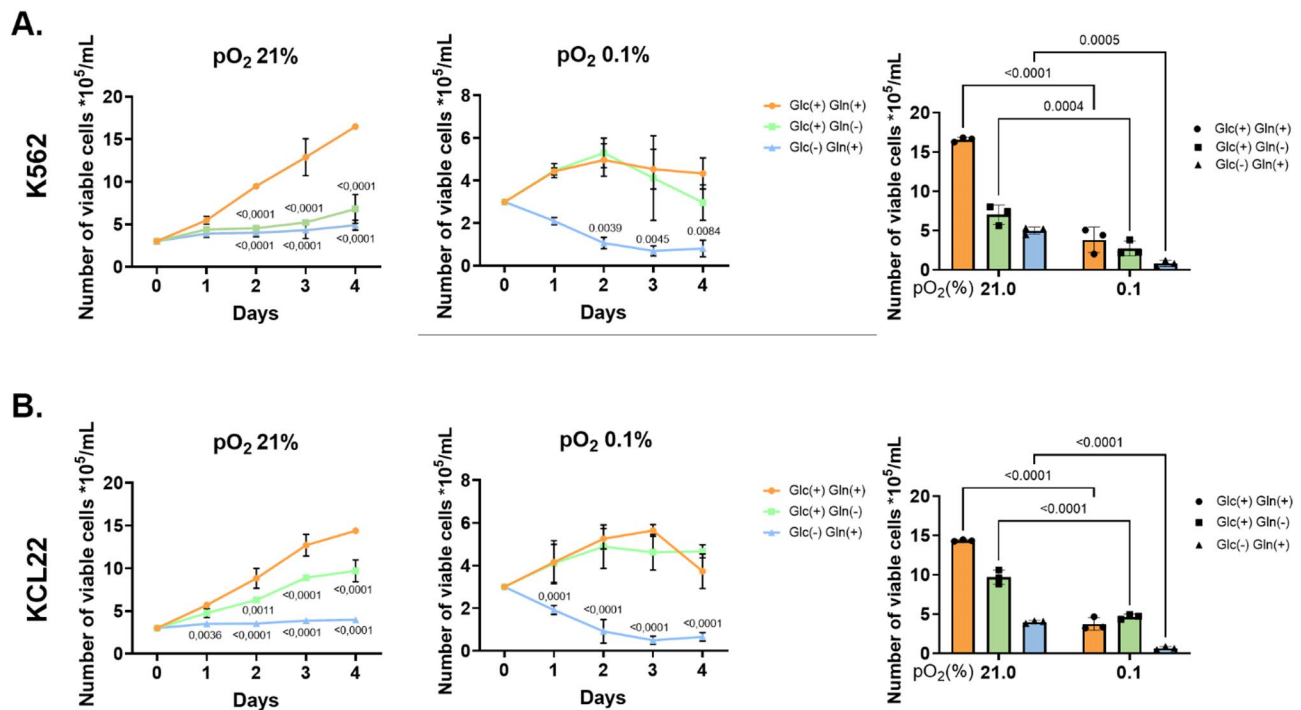


Fig. 1 Effects of glucose and/or glutamine on CML cell survival and proliferation. K562 (A) and KCL22 (B) cells were subjected to Glc and/or Gln deprivation for 4 days under low oxygen (0.1% O₂) or standard conditions (21.0% O₂), whereas cells in complete medium (Glc+/Gln+) were used as controls. Trypan blue-negative cells were counted at the indicated incubation times (left and middle panels), and the final results (day 4) are shown in the right panels. Data are expressed as the mean \pm SD of the data from three independent experiments ($n=3$). The differences for which statistical significance is indicated in the left and middle panels are with respect to Glc+/Gln+ while on the right panels, the statistical significance was calculated for Normoxia Vs Hypoxia samples

limit before the ignition of cell stress due to excessive Glc consumption.

Glutamine enhances glycolytic capacity

Seahorse assays showed that Gln enhanced Glc consumption, as Glc+/Gln+ cultures yielded higher levels of glycolytic capacity than Glc+/Gln- cultures (Fig. 2). The higher glycolytic capacity of Glc+/Gln+ cultures reflects the higher proliferation level, as shown in Fig. 1, as glycolysis is probably the most important metabolic event sustaining cell cycling and proliferation. Being glycolysis and glutaminolysis interconnected events, we can state that the Gln exhibits the potential to enhance glycolysis. While the Seahorse method includes Glc in the assay medium, we want to emphasize that the enhancing effect of Gln is observed under physiological conditions only when glucose is available. It should be noted that in low oxygen, Glc+/Gln- and Glc-/Gln+ cultures showed a significantly higher level of non-glycolytic acidification than Glc+/Gln+ cultures. Such acidification has been reported [26] to be affected by the consumption of intracellularly stocked metabolites, such as glycogen and FA, which might be synthesized during the first days of oxygen deprivation and consumed after all other nutrients available in the culture medium are exhausted.

The lack of oxygen affects cell metabolic demand

To better assess the contribution of Glc and Gln to the oxidative phosphorylation and the CML metabolic dependencies in normoxic and hypoxic conditions we measured K562 and KCL22 OCR through the Seahorse platform. Gln was found to be capable of inhibiting oxidative phosphorylation, as both the basal and maximal respiration rates were higher in Glc+/Gln- cultures than in the other experimental conditions, in both “normoxia” and low oxygen (Fig. 3A, B). Moreover, as demonstrated in Fig. 3C by the Mito Fuel Dependency Test, cells incubated in low oxygen conditions developed a higher dependency on FA oxidation, which might be associated with the previously observed non-glycolytic acidification.

Glutamine stimulates lipid storage in the absence of glucose

To investigate the presence of observable signs of metabolite storage that might be responsible for the previously observed non-glycolytic acidification, we subjected CML cells incubated in “normoxia” or low oxygen to TEM imaging. As shown in Fig. 4, several LDs are clearly observable in Glc-/Gln+ cells as round opaque objects. Although some LDs were detectable even under normoxic conditions, incubation in low oxygen conditions

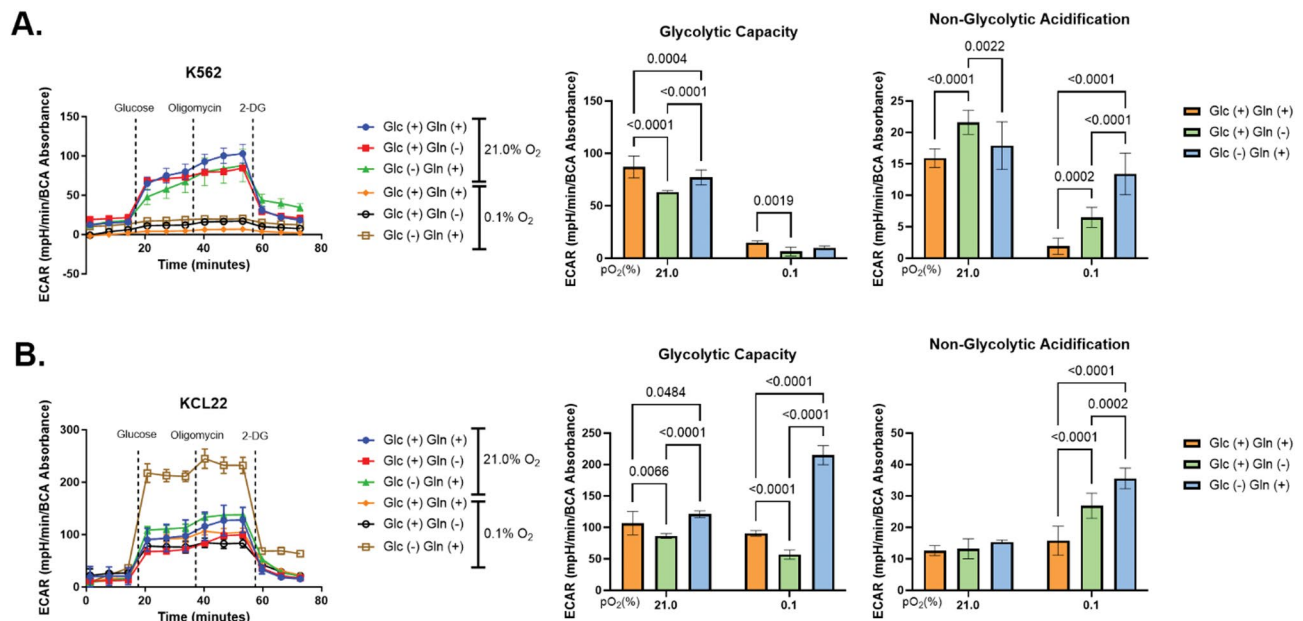


Fig. 2 Glutamine enhances glycolytic capacity. Cells were incubated as indicated for four days and then subjected to the GlycoStress assay. The ExtraCellular Acidification Rate (ECAR) measured (**A**, K562; **B**, KCL22) is shown as complete patterns obtained from representative Seahorse runs (left panels) or as the average of independent measures (middle and right panels). The correlation between EACR and intracellular and extracellular lactate production is shown in Supplementary Fig. 1E. The latter data are expressed as the mean \pm SEM of the results from at least three independent experiments, each consisting of cell plating into six Seahorse microplate wells ($n=3$)

resulted in the formation of a much higher number of larger LDs. Thus, in the absence of Glc, Gln markedly stimulates lipid storage, especially under low oxygen conditions.

Glutamine induces FA accumulation

While TEM allowed us to observe LDs formation, this is neither a specific nor a quantitative method for lipid quantification. Therefore, to validate and measure LDs formation induced in Glc-/Gln+ cultures incubated in “normoxia” or low oxygen, CML cells were stained with BODIPY 493/503 and analyzed using flow cytometry and confocal microscopy (Fig. 5A and B, respectively). In low oxygen and in the absence of Glc, the presence of Gln significantly increased neutral lipid accumulation in the form of LDs (Fig. 5A, B). To better assess the contribution of Gln to FA accumulation, we performed a GC/MS experiment using ¹³C₅-labeled Gln. As shown in Fig. 5C, the most common long-chain FA (palmitic, oleic, and stearic acids) were not produced by *de novo* synthesis from Gln synthesis. Therefore, Gln is responsible for neutral lipids accumulation in the form of LDs inside the cells but it is not an intermediate metabolite in FA production.

CD36-mediated FA uptake induces a block of *de novo* FA synthesis

The above results show that intracellular lipid accumulation is mediated by Gln, but the resulting FA is not directly derived from Gln itself. Indeed, *de novo* synthesis

of FA is an energy-consuming mechanism that involves a significant amount of Krebs cycle intermediates which are less produced under oxygen deprivation. Therefore, we explored the possibility of Gln-driven uptake in the extracellular milieu. Among the several described FA importers, CD36, alias FA Translocase (FAT), plays a major role in the uptake of low-density lipoproteins and long-chain FA, especially in CML cells [27]. To determine whether CD36 is involved in the observed FA accumulation, we evaluated its expression using flow cytometry. As shown in Fig. 6A, CD36 expression levels were increased in Glc-/Gln+ cultures incubated in low oxygen only, compared to all other experimental variants. Figure 6B links such CD36-mediated FA accumulation to a block of the *de novo* synthesis of FA via a negative feedback loop, as suggested by the reduced expression of the main enzyme involved in FA synthesis (FA-synthase). In these experiments, BCR::ABL1 (p210) was found to be downregulated in low oxygen conditions in the presence of Gln and much less in its absence. Thus, under oxygen/Glc shortage, Gln appears to enhance FA uptake and oxidation in CML cells, where the BCR::ABL1 protein is suppressed.

FA interfere with BCR::ABL1 expression and the maintenance of stem cell potential

To reconnect the above-described findings relative to FA to the expression of the BCR::ABL1 protein, exogenous BSA-palmitate was added to Glc+/Gln- cultures. Where FA accumulation was not observed and the maintenance

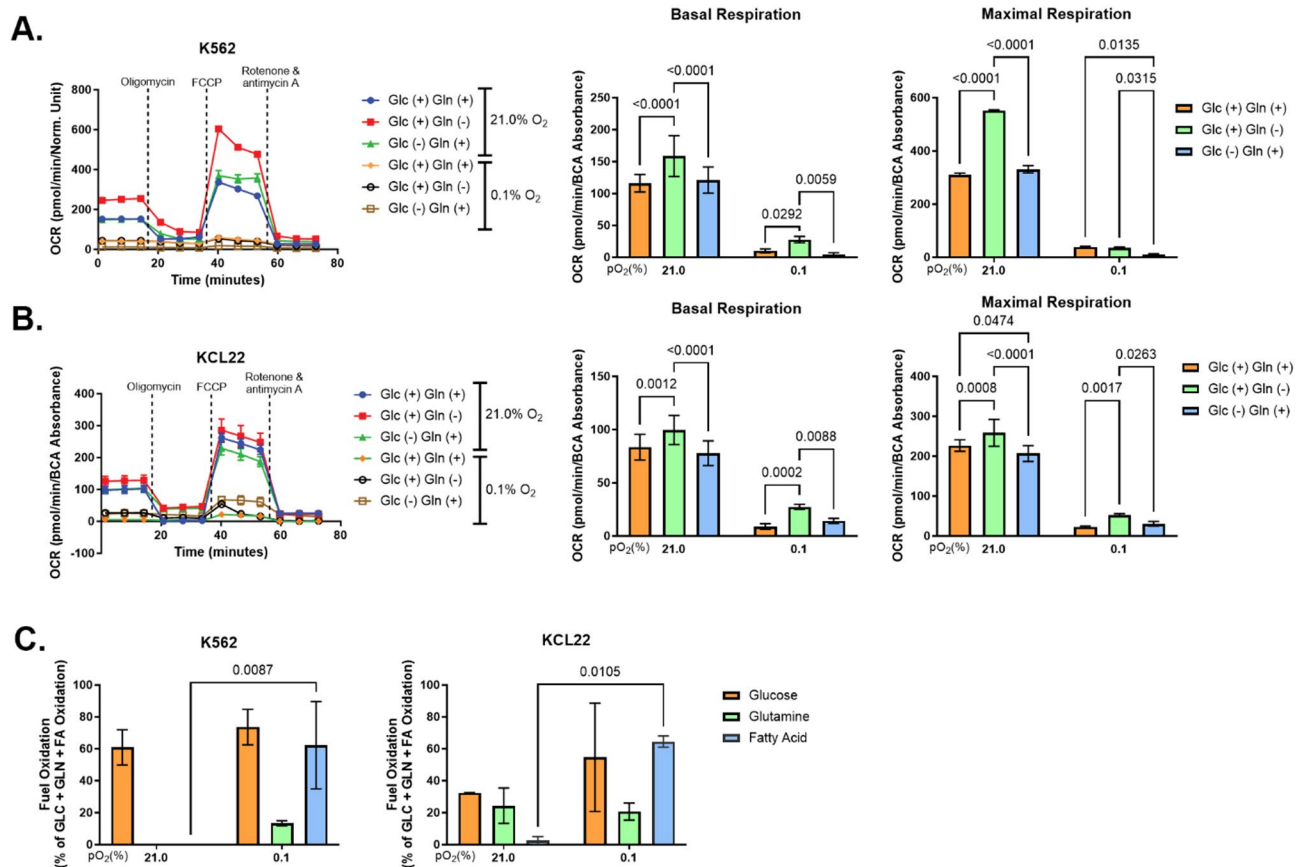


Fig. 3 The lack of oxygen affects cell metabolic demand. Cells were incubated as indicated for 4 days and then subjected to MitoStress or Mito Fuel Flex assays. The Oxygen Consumption Rate (OCR) measured by the mitostress test (**A**, K562; **B**, KCL22) is shown as complete patterns obtained from representative Seahorse runs (left panels) or as the average of independent measures (middle and right panels). The Fuel Oxidation Dependency (**C**) was calculated using the following equation: $\text{Dependency \%} = \left[\frac{\text{Baseline OCR} - \text{Target Inhibitor OCR}}{\text{Baseline OCR} - \text{All inhibitors OCR}} \right] * 100$. Only the oxidation dependence of FA was statistically significant. Averaged data are expressed as the mean \pm SEM of results from at least three independent experiments, each consisting of cell plating into six Seahorse microplate wells ($n = 3$)

of BCR::ABL1 expression was usually boosted, BSA-palmitate inhibited this expression in both “normoxia” and low oxygen (Fig. 7A). In contrast, when Glc-/Gln+ cultures, where FA accumulation was favored, were treated with a specific CD36 inhibitor, sulfo-N-succinimidyl oleate [28] (SSO), an analog long-chain FA that inhibits FA transport into cells, BCR::ABL1 expression was enhanced (Fig. 7B). This enhancement corresponded to the increased biological activity of BCR::ABL1, as determined by CrkL phosphorylation (Fig. 7C). Thus, intracellular accumulation of exogenous FA inhibits BCR::ABL1 protein expression and signaling.

To assess whether the FA-dependent modulation of BCR::ABL1 protein expression affects the maintenance of stem/progenitor cell potential, Glc-/Gln+ cultures were incubated for 4 days in low oxygen in the absence or presence of SSO and then subjected to the CRA assay. As a further control, etomoxir, an inhibitor of FA β -oxidation that forces cells to maintain a high level of intracellular lipids, was added to the normoxia-incubated, unselective,

growth-permissive cultures (LC2) of the CRA assay, where the stem cell potential rescued from the selective experimental cultures (LC1) was exploited (Fig. 7D). The inhibition of FA uptake accelerated LC2 repopulation (see SSO-treated vs. control and day 5 vs. day 13). In contrast, the inhibition of β -oxidation reduced the cumulative (at the end of incubation) LC2 repopulation (see Etomoxir-treated vs. control and day 13 vs. day 5). Thus, the low lipid content of cells endowed with stem/progenitor cell potential favors the maintenance of BCR::ABL1-dependent stem cell potential, the actualization of which relies on lipid consumption via β -oxidation. This indicates that the availability and consumption of lipids are detrimental to the maintenance of BCR::ABL1-dependent stem cell potential.

CML cells stimulate BM adipocytes to secrete FA

Finally, to match the features of SCN, namely the interaction of HSC/LSC with stromal SCN cells, we co-cultured CML cells with HS27A cells, the latter induced to

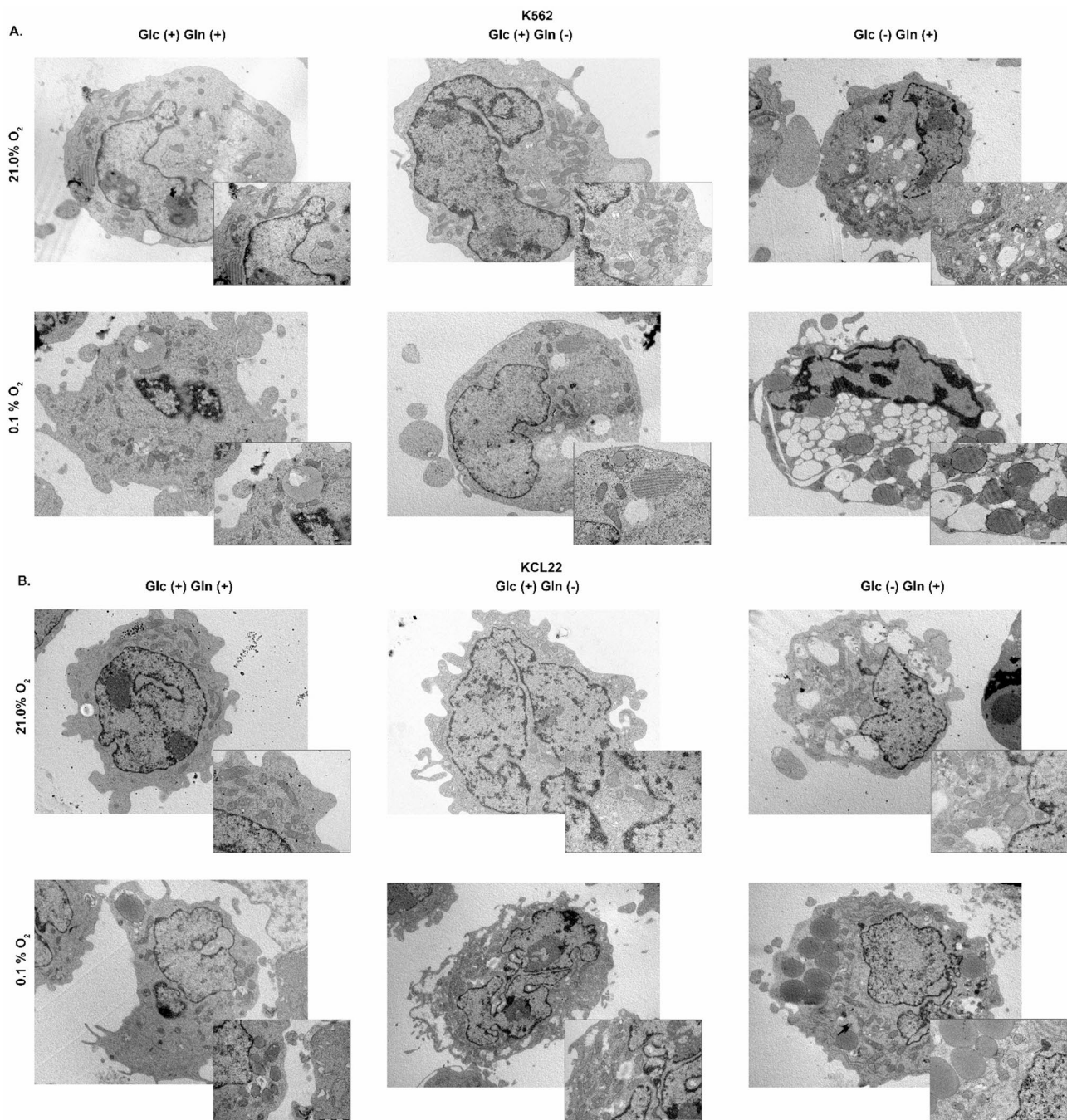


Fig. 4 Glutamine stimulates lipid storage in the absence of glucose. K562 (A) and KCL22 (B) cells were incubated as indicated for four days and then fixed and prepared for TEM analysis. Images were captured using a JEM 1010 transmission electron microscope equipped with a MegaView III high-resolution digital camera ($n=3$)

adipocyte differentiation using a specific medium (see Materials and Methods). Preliminary to the co-culture, HS27A cells that were induced to differentiate into adipocytes were subjected to three different metabolic conditions. When Gln- HS27A adipocyte cultures were incubated in low oxygen for 4 days, FABP4 and PPAR γ , two main markers of BM adipocyte maturation [29], were maximally upregulated (Fig. 8A). The lack of Gln also

induced HS27A adipocytes to the maximal secretion of neutral lipids in the culture medium, as determined by Nile Red staining (Fig. 8B). In contrast, when HS27A adipocytes were co-cultured with CML cells, FABP4 and PPAR γ expression in adipocytes was enhanced in all cases, but the presence of Gln maximized this enhancement independently of the absence or presence of Glc (Fig. 8C). Thus, CML cells, which reach maximum FA

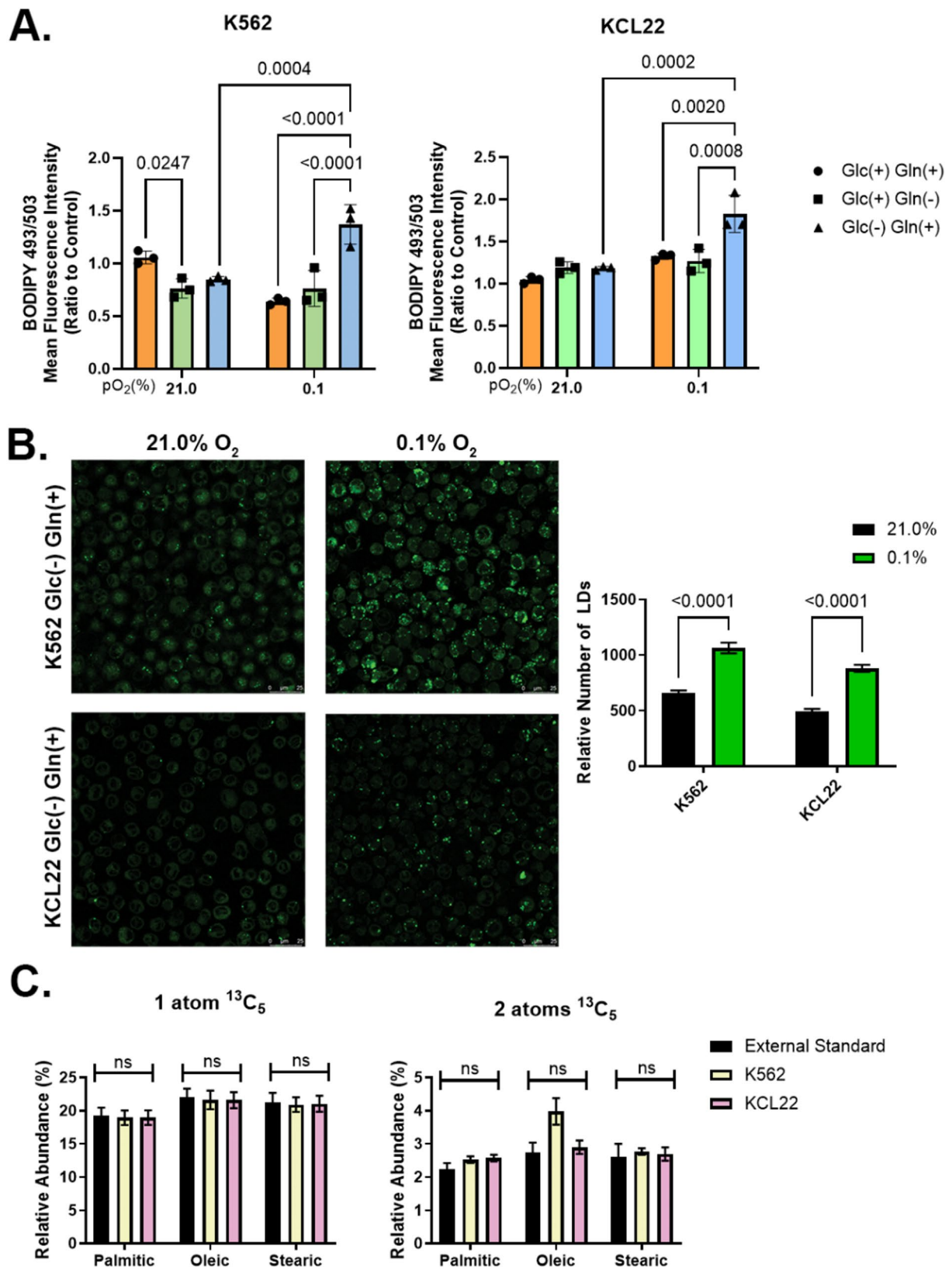


Fig. 5 (See legend on next page.)

(See figure on previous page.)

Fig. 5 Glutamine induces FA accumulation. K562 and KCL22 cells were incubated as indicated for 4 days, stained with BODIPY 493/503, and analyzed by flow cytometry (A) and confocal analysis (B). For the latter, an algorithm to count green positive pixels was exploited on 60 z-stack slices to include the entire cell volume. The graph in (B) shows the total number of identifiable LDs in the examined slides. (C) Cell content of palmitic, oleic, and stearic acids, as determined by GC/MS using $^{13}\text{C}_5$ -labeled Gln and tracing 1 or 2 Gln-derived carbon atoms. Data are expressed as the mean \pm SD of the data from three independent experiments ($n=3$)

uptake in the presence of Gln, induce adipocytes to enhance the expression of FABP4 and PPAR γ (stimulating triacylglycerol synthesis and lipogenesis and enhancing the influx of extracellular FA [15]), within a scenario of metabolic symbiosis.

Discussion

CML is a monogenic disease in which BCR::ABL1 plays a major role in all pathological aspects and its modulation is closely dependent on the availability of microenvironmental nutrients. The absence of one of the major sources of energy and biomaterial production, Glc and Gln, significantly affects not only cell viability and proliferation but also the expression levels of the BCR::ABL1 oncoprotein. In our study, we demonstrated that Glc alone (without Gln), while partially supporting cell growth under “normoxia,” is crucial for cell growth under low-oxygen conditions, whereas Gln alone (without Glc) is incapable of supporting cell growth under either condition. In combination with Glc, Gln enhances cell growth under normoxia, but it is irrelevant under low-oxygen conditions. The fact that Glc is indispensable in low oxygen conditions is consistent with cell adaptation to environmental conditions, where the TCA cycle is strongly inhibited due to the scarce availability of oxygen, which is an electron donor-acceptor; therefore, cells rely on Glc availability and glycolysis as the main pathway of energetic metabolism [30].

In keeping with the observed enhancement of cell growth in normoxia, Gln was shown to downregulate the respiratory activity to enhance glycolysis, likely due to the regulatory effect of Gln on mTORC1, which is reportedly one of the main orchestrators of glycolysis, mitochondrial biosynthesis, and cell proliferation [31]. In low oxygen Gln, despite the lack of an effect on cell growth, it was far from irrelevant. Gln enhances FA metabolism, being responsible for the so-called “non-glycolytic acidification”, which is commonly generated by β -oxidation and glycogenolysis and is markedly upregulated under Glc and oxygen shortage [26, 32]. Thus, we investigated the metabolic rewiring imposed by the presence of Gln in low oxygen conditions and identified a significant accumulation of FA in the form of LDs occurring in the absence of Glc. Indeed, FA are commonly rapidly activated by coenzyme A (CoA) to form fatty acyl-CoA, which then combines with glycerol to generate TAG. In this stable form, FA are stored in LDs, which are one of

the main storage sites mobilized by cells for ATP production and biomaterial accumulation [33].

In keeping with FA accumulation, we also found that Gln is capable of inducing the CD36-mediated uptake of extracellular FA, which, on the one hand, drives the downregulation of BCR::ABL1 oncoprotein; on the other hand, it represents a reserve of energy to trigger clonal expansion once the oxygen concentration is increased and growth-permissive conditions are established. In this way, Gln renders CML cells, thanks to BCR::ABL1 suppression, capable of surviving under oxygen/Glc shortage, i.e. to be hosted in the “core” of our SCN model where stem cell potential is maintained and clonal expansion is restrained. However, these cells are energetically ready to rapidly proliferate once they move to the outer zone of the SCN, where BCR::ABL1 re-expression is allowed. This is consistent with the results obtained by Bensaad et al., who showed that FA accumulation in the form of LDs occurs under oxygen shortage via HIF-1 α in a time- and oxygen concentration-dependent manner, and contributes to cell survival and growth during the reoxygenation phase [17]. The accumulation of external FA triggers the downregulation of *de novo* FA synthesis, decreasing FASN, probably triggering β -oxidation instead. This is coherent also with the data obtained by Fuhrmann et al., who demonstrated that, when oxygen shortage becomes chronic, the cells behave in a “normoxic” way, by actively oxidizing FA and Gln via the overexpression of electron-transferring flavoproteins [34]. On this basis, we blocked CD36 via the specific inhibitor SSO, which has been reported to hamper the proliferation of cancer cells [35, 36], demonstrating that FA is fundamental for BCR::ABL1 downregulation under both low oxygen and normoxia. CrkL was specifically chosen as a readout for BCR::ABL1 activity because it is one of its key downstream signaling effectors and a well-established surrogate marker of BCR::ABL1 kinase activity in CML. Given our findings that FA metabolism influences BCR::ABL1 expression, we further validate the link between lipid metabolism and BCR::ABL1 signaling and its potential impact on LSC maintenance [37].

To our knowledge, direct studies focused on CML on the specific pathways with the particular conditions treated in the present manuscript are limited. However, being hypoxia a conditions which fuel TKi resistance, by suppressing the expression of the oncoprotein BCR::ABL1 and allowing CML cells to enter a quiescent status, we observed a strong parallelism with two

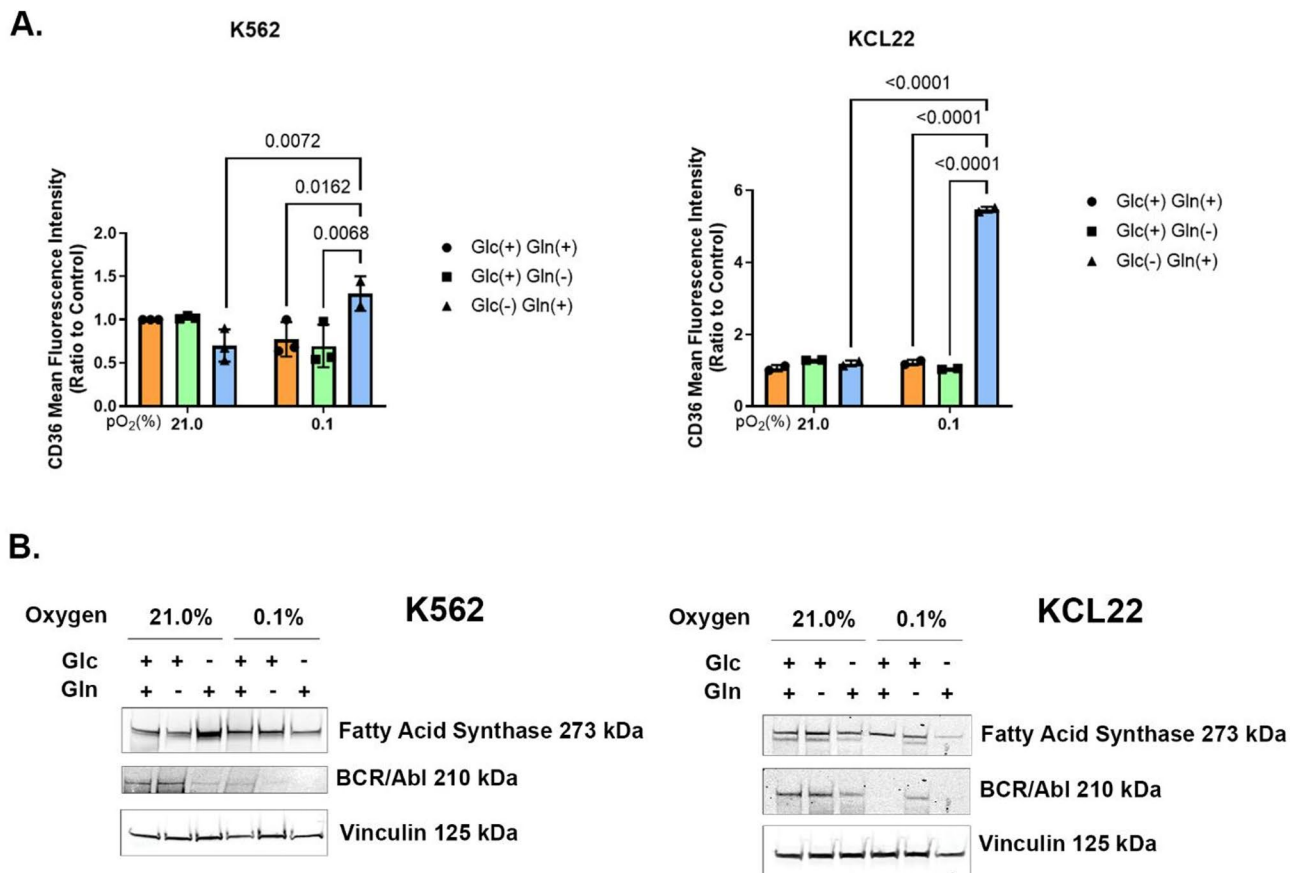


Fig. 6 CD36-mediated FA uptake induces a block of *de novo* FA synthesis. K562 and KCL22 cells were incubated for 4 days as indicated. **(A)** CD36 expression was measured by flow cytometry. Glc(-) Gln(+) in hypoxia was compared only to Glc(+) Gln(+) and Glc(+) Gln(-) in the same oxygen condition, and versus Glc(-) Gln(+) in normoxia **(B)** Total cell lysates were subjected to immunoblotting to determine the expression levels of FA-synthase and BCR::ABL1. The loading of equal amounts of vinculin protein was confirmed by immunoblotting and the average densitometric values of bands from three independent experiments, obtained using ImageJ software, are reported in Supplementary Fig. 1A. Data reported in (A) are expressed as the mean \pm SD of the data from three independent experiments ($n = 3$)

specific studies: in accordance with our model, Mostazo et al. demonstrated that Gln, by contributing to proline synthesis, is fundamental in the process of gaining chemoresistance to TKi, in both hypoxic and normoxic conditions [38]. In this context, it is now widely reported that imatinib exposure leads to alterations in fatty acid synthesis in BCR::ABL1-positive cell lines [39–41]. Moreover, Salaverry et al. by studying K562 cells exposed to oxygen concentration lower than 1% demonstrated that mitochondria are not a significant source of ATP, and HIF is capable of triggering their elimination through a mitophagic response. In accordance with our study, they observed that the few mitochondria remained rerouted their operational way, increasing citrate efflux, showing a truncated form of the Krebs cycle, and increasing fatty acid synthesis and cholesterol homeostasis-associated gene expression [42].

To deepen the relationship between CML cells and the BM microenvironment, we considered adipocytes, which represent the main reservoir of FA storage, by making

them serve as a feeder layer [43]. Indeed, in *in vitro* conditions, free FA are commonly provided by FBS or by external sources like BSA-Palmitate. However, under physiological conditions, FA for CML cells within the BM niche are primarily supplied by the large pool of adipocytes that colonize the BM [44]. By co-culturing CML cells with mature adipocytes, we found that when Gln is available in low oxygen, CML cells induce upregulation of FABP4 and PPAR γ , markers of BM adipocyte maturation [29], and stimulation of TAG synthesis, lipogenesis, and extracellular FA influx [15]. This is an important phenomenon, consistent with previous studies reporting that adipocytes, through FA release, induce maintenance of the LSC compartment [45]. Ye et al. also demonstrated that an LSC subset of AML and CML is preferentially located in extramedullary adipose niches and over-expresses CD36 [46], validating the close relationship between the maintenance of stem status and the secretory action of BM adipose tissue.

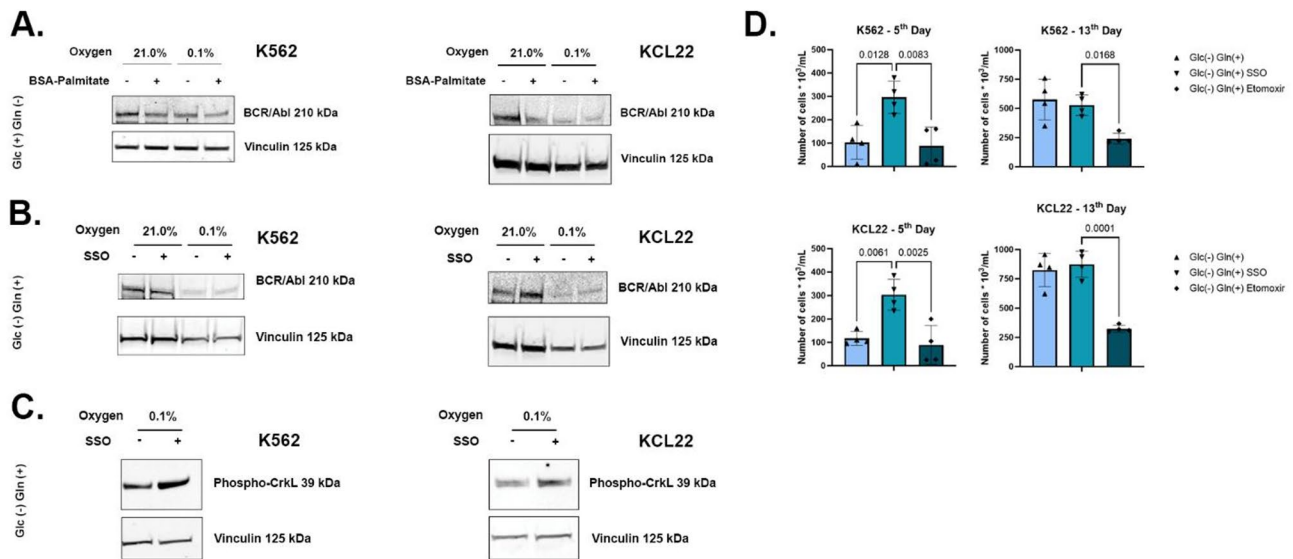


Fig. 7 FA interfere with BCR::ABL1 expression and the maintenance of stem cell potential. K562 and KCL22 cells were incubated as indicated for 4 days and treated from time zero of incubation with BSA-Palmitate (ratio 1:8–100 μM) in the presence of Glc only (**A**) or with SSO (150 μM) in the presence of Gln only (**B, C**). Total cell lysates were subjected to immunoblotting to determine the expression levels of BCR::ABL1 and phospho-Crk, as well as vinculin, to confirm the loading of equal amounts of protein. The average densitometric values of bands from three independent experiments, obtained using ImageJ software, are reported in Supplementary Figs. 1B, C, and D, respectively. In (**D**), cells incubated for 4 days in low oxygen (LC1) in the absence or presence of SSO from time 0 of LC1 incubation were replated into growth-permissive cultures established in complete growth medium and incubated in normoxia (LC2) in the absence or presence of etomoxir from time 0 of LC2 incubation. Trypan blue-negative cells were counted after 5 (left panels) or 13 (right panels) days of incubation in LC2 medium. Data are expressed as the mean \pm SEM of data from four independent experiments ($n = 3$)

Although very few studies reporting the role of lipid metabolism in CML have been published to date, Gonzalez et al. described that the impairment of glycerophospholipid metabolism due to the loss of G0/G1 switch gene 2 (G0S2) promotes CML progression and drug resistance [47], while Naka et al. showed that the lysophospholipase D enzyme Glycerophosphodiester Phosphodiesterase Domain Containing 3 (Gdpd3), a key enzyme in the hydrolysis of the polar base of lysophospholipids, such as choline, ethanolamine, inositol, and serine, is critical for the long-term maintenance of CML stem cells by activating stemness factors such as Foxo3a and β -catenin [48]. It's important to note that the clinical application of targeting lipids and FA pathways in CML still remains under investigation. Ricciardi et al. reported, in a brief report, the antileukemic activity of the novel CPT1a inhibitor ST1326 on several leukemia cell lines and primary cells, demonstrating that it was capable of determining cell growth arrest, mitochondrial damage, and apoptosis induction, in particular on acute myeloid leukemia cells. Even suggesting that leukemia cells might be affected by targeting the FA oxidation pathway they conducted their work only on acute myeloid leukemia (AML), acute lymphoblastic leukemia (B-ALL), and chronic lymphoblastic leukemia (CLL) and not on CML [49]. More recently, it was reported that the combined use of venetoclax and dasatinib in blast-phase CML is capable of upregulating the expression of the lysosomal acid lipase A (LIPA), a

key regulator of free fatty acids. Minhajuddin et al. confirmed indeed an increased level of free FA in response to treatment with venetoclax/dasatinib and by pretreating leukemia cells with bafilomycin, a specific lysosome inhibitor, or by silencing the LIPA gene, they also demonstrated an increased sensitivity of leukemia cells to venetoclax/dasatinib, providing a rationale for free FA regulation as an adjunctive therapeutic strategy to prolong disease remission [50]. Another research group explored a preclinical approach on the theme: Shinohara et al. reported that a FA derivative, AIC-47, induced transcriptional repression of the BCR::ALB1 gene and modulated the expression profile of the Pyruvate Kinase M1/2, ultimately leading to autophagic cell death. AIC-47 altered the PPAR γ / β -catenin pathway, down-regulated c-Myc, disrupted the BCR::ALB1/mTOR/hnRNP signaling axis, and induced a switch from PKM2 to PKM1 expression, causing autophagic cell death via increased ROS level [51]. Their evidence of a FA derivative which has the potential to decrease BCR::ABL1 is in line with what we demonstrated by using Palmitate, as the most simple FA available, and by treating cells with SSO: the more abundant is the storage of FA inside the cell, the less is BCR::ABL1 expression. To date, to our knowledge, the only one clinical trial involving FA pathway modulation in CML patients was conducted by the Milton S. Hershey Medical Center by daily administering Eicosapentaenoic Acid (EPA) in combination with a TKi. This

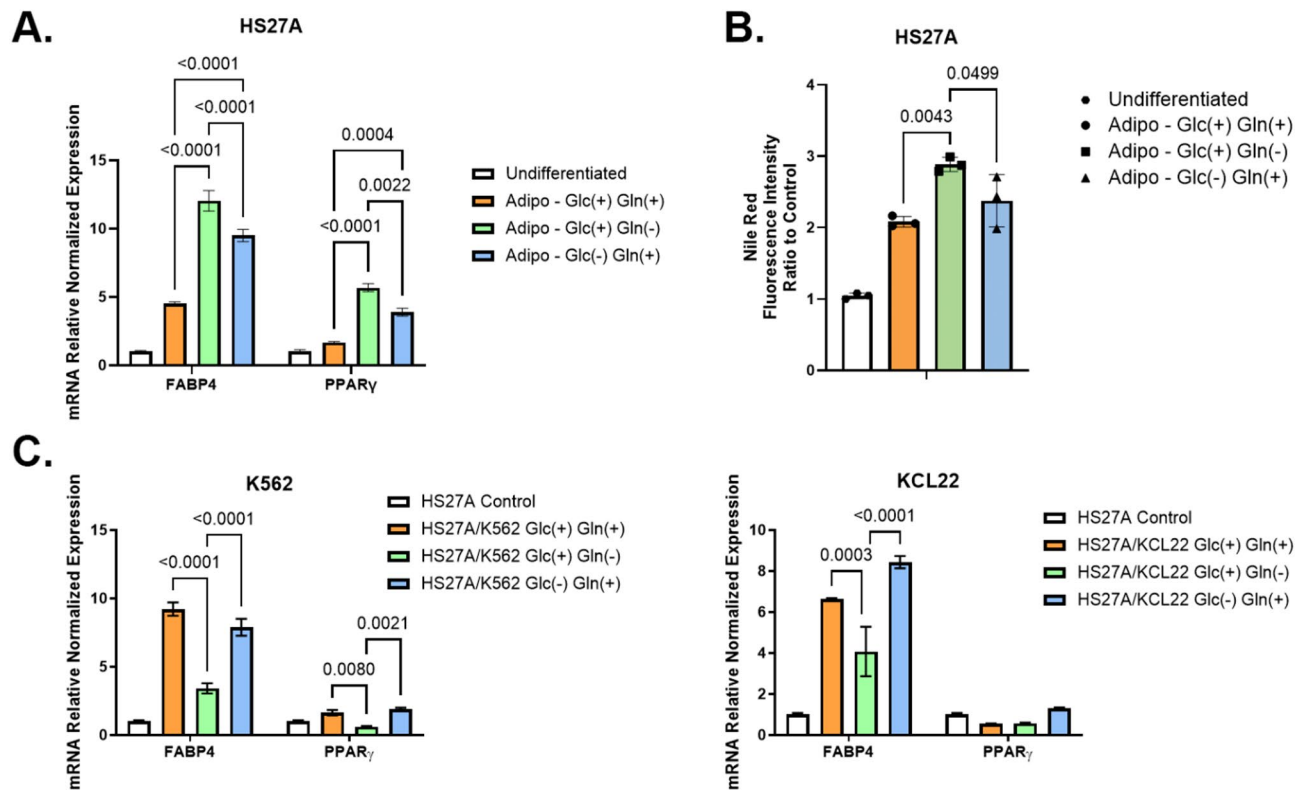


Fig. 8 CML cells stimulate BM adipocytes to secrete FA. Total RNA isolated using Tri Reagent from HS27A cells previously differentiated into adipocytes, alone (A) or co-cultured with CML cells (C), was subjected to RT, and qPCR was performed for FABP4 and PPAR γ normalized by comparison with three different housekeeping genes (GAPDH, 18 S, and ACTB). (B) Conditioned media from differentiated HS27A cells were collected and the neutral lipid content was evaluated by Nile Red staining. All experiments were performed with cells incubated in low oxygen for four days. Data are expressed as the mean \pm SD of data from at least three independent experiments ($n = 3$)

study included both a Phase 1, determining the safety of the EPA in chronic stable phase patients, and a Phase 2 component, testing the maximum tolerated dose (MTD), planning also to examine the anti-CML effects of EPA when administered with a TKI [NCT04006847]. Unfortunately, the trial was terminated after enrolling only one participant, limiting the conclusions that could be drawn from it.

Conclusions

Taken together, our findings strengthen the hypothesis of a central role of FA in the maintenance of the LSC compartment in CML, demonstrating, for the first time, the relationship between FA and BCR::ABL1 oncoprotein expression and the pivotal role of Gln in the regulation of FA uptake as a metabolic mechanism capable of maintaining CML in the restrictive conditions of SCN, yet preparing the cells for clonal expansion once these restrictions are released. We are aware of the limitation of our study about the lack of patient-derived samples; the isolation of CML cells from BM, where they persist within the SCN into severe hypoxic conditions, represents a significant logistic and technical challenge, in particular maintaining continuously the lack of oxygen,

avoiding in that way bias due to the reoxygenation generated ROS. Moreover, the collection of such samples requires invasive procedures and limited ethical approvals thus, the availability of freshly isolated CML cells is often limited. Additionally, primary CML cells, in particular the ones residing in the hypoxic BM niche, exhibit heterogeneity and variable responses, necessitating optimized and standardized protocols. However, our study for the first time highlights the role of Gln in facilitating lipid uptake and oxidation, suggesting that metabolic interventions could be used to disrupt leukemia cell adaptation. In particular, inhibiting FA uptake via CD36 blockade (e.g., with SSO) or targeting β -oxidation (e.g., with Etomoxir) may prevent the metabolic rewiring that supports LSC maintenance or clonal expansion, respectively. Furthermore, disrupting the metabolic symbiosis between CML cells and BM adipocytes could limit the tumor-supportive microenvironment, potentially enhancing treatment efficacy. These insights provide a rationale for combining metabolic inhibitors with existing CML therapies, particularly in patients with resistance to TKI or in targeting the pool of LSC to prevent relapse.

Supplementary Information

The online version contains supplementary material available at <https://doi.org/10.1186/s12935-025-03805-y>.

Supplementary Material 1

Acknowledgements

Not applicable.

Author contributions

C.M. performed the investigation and developed the needed methodology and protocols; G.M. and S.P. supported C.M. in the optimization of several methods and in collecting materials; G.V. validated the analysis. D.G. performed the TEM analysis; G.P. performed the GC/MS investigation; R.E. and L.P. collected fundamental resources; M.L. supported the conceptualization of the study; P.D.S. supported the conceptualization of the study, wrote the original draft, supervised the personnel and was responsible for funding administration and acquisition. A.B. supported the conceptualization of the study, wrote the original draft, was responsible for the analysis, figure preparation and for the project investigation.

Funding

This project was supported by the Fondazione Associazione Italiana per la Ricerca sul Cancro (AIRC) grant IG23607/2019 (PDS). AB and SP were supported by postdoctoral fellowships funded by Fondazione Pezcoller and Fondazione Veronesi, respectively.

Data availability

No datasets were generated or analysed during the current study.

Declarations

Ethics approval and consent to participate

Not applicable.

Consent for publication

Not applicable.

Competing interests

The authors declare no competing interests.

Author details

¹Department of Experimental and Clinical Biomedical Sciences "Mario Serio", Università degli Studi di Firenze, Florence, Italy

²Department of Experimental and Clinical Medicine, Università degli Studi di Firenze, Florence, Italy

³CISM Mass Spectrometry Center, Università degli Studi di Firenze, Florence, Italy

Received: 2 January 2025 / Accepted: 4 May 2025

Published online: 14 May 2025

References

1. Busch C, Mulholland T, Zagnoni M, Dalby M, Berry C, Wheadon H. Overcoming BCR:ABL1 dependent and independent survival mechanisms in chronic myeloid leukaemia using a multi-kinase targeting approach. *Cell Commun Signal*. 2023;21:342.
2. Cheloni G, Tanturli M, Tusa I, Ho DeSouza N, Shan Y, Gozzini A, et al. Targeting chronic myeloid leukemia stem cells with the hypoxia-inducible factor inhibitor acriflavine. *Blood*. 2017;130:655–65.
3. Holyoake TL, Vetrie D. The chronic myeloid leukemia stem cell: stemming the tide of persistence. *Blood*. 2017;129:1595–606.
4. Challen GA, Goodell MA. Clonal hematopoiesis: mechanisms driving dominance of stem cell clones. *Blood*. 2020;136:1590–8.
5. Chen J, Kang J-G, Keyvanfar K, Young NS, Hwang PM. Long-term adaptation to hypoxia preserves hematopoietic stem cell function. *Exp Hematol*. 2016;44:866–e8734.
6. Cheloni G, Poteti M, Bono S, Masala E, Mazure NM, Rovida E, et al. The leukemic stem cell niche: adaptation to hypoxia versus oncogene addiction. *Stem Cells Int*. 2017;2017:4979474.
7. Silvano A, Menegazzi G, Peppicelli S, Mancini C, Biagioni A, Tubita A, et al. Lactate maintains BCR/Abl expression and signaling in chronic myeloid leukemia cells under nutrient restriction. *Oncol Res*. 2022;29:33–46.
8. Bono S, Lulli M, D'Agostino VG, Di Gesualdo F, Loffredo R, Cipolleschi MG, et al. Different BCR/Abl protein suppression patterns as a converging trait of chronic myeloid leukemia cell adaptation to energy restriction. *Oncotarget*. 2016;7:84810–25.
9. Rovida E, Peppicelli S, Bono S, Bianchini F, Tusa I, Cheloni G, et al. The metabolically-modulated stem cell niche: a dynamic scenario regulating cancer cell phenotype and resistance to therapy. *Cell Cycle*. 2014;13:3169–75.
10. Mazat J-P, Ransac S. The fate of glutamine in human metabolism. The interplay with glucose in proliferating cells. *Metabolites*. 2019;9:81.
11. Poteti M, Menegazzi G, Peppicelli S, Tusa I, Cheloni G, Silvano A, et al. Glutamine availability controls BCR/Abl protein expression and functional phenotype of chronic myeloid leukemia cells endowed with stem/progenitor cell potential. *Cancers*. 2021;13:4372.
12. Wappler J, Arts M, Röth A, Heeren RMA, Peter Neumann U, Olde Damink SW, et al. Glutamine deprivation counteracts hypoxia-induced chemoresistance. *Neoplasia*. 2020;22:22–32.
13. Yoo HC, Yu YC, Sung Y, Han JM. Glutamine reliance in cell metabolism. *Exp Mol Med*. 2020;52:1496–516.
14. Fuhrmann DC, Brüne B. Mitochondrial composition and function under the control of hypoxia. *Redox Biol*. 2017;12:208–15.
15. Mylonis I, Simos G, Paraskeva E. Hypoxia-inducible factors and the regulation of lipid metabolism. *Cells*. 2019;8:214.
16. Blum JL, Bijli KM, Murphy TC, Kleinhenz JM, Hart CM. Time-dependent PPAR γ modulation of HIF-1 α signaling in hypoxic pulmonary artery smooth muscle cells. *Am J Med Sci*. 2016;352:71–9.
17. Bensaad K, Favaro E, Lewis CA, Peck B, Lord S, Collins JM, et al. Fatty acid uptake and lipid storage induced by HIF-1 α contribute to cell growth and survival after hypoxia-reoxygenation. *Cell Rep*. 2014;9:349–65.
18. Hu B, Guo Y, Garbacz WG, Jiang M, Xu M, Huang H, et al. Fatty acid binding protein-4 (FABP4) is a hypoxia inducible gene that sensitizes mice to liver ischemia/reperfusion injury. *J Hepatol*. 2015;63:855–62.
19. Durandt C, van Vollenstee FA, Dessels C, Kallmeyer K, de Villiers D, Murdoch C, et al. Novel flow cytometric approach for the detection of adipocyte subpopulations during adipogenesis. *J Lipid Res*. 2016;57:729–42.
20. Hammel JH, Bellas E. Endothelial cell crosstalk improves browning but hinders white adipocyte maturation in 3D engineered adipose tissue. *Integr Biol (Camb)*. 2020;12:81–9.
21. Andreucci E, Biagioni A, Peri S, Versienti G, Cianchi F, Staderini F, et al. The CAIX inhibitor SLC-0111 exerts anti-cancer activity on gastric cancer cell lines and resensitizes resistant cells to 5-fluorouracil, taxane-derived, and platinum-based drugs. *Cancer Lett*. 2023;571:216338.
22. Dello Sbarba P, Cheloni G. Tissue hypoxia and the maintenance of leukemia stem cells. *Adv Exp Med Biol*. 2019;1143:129–45.
23. Bono S, Dello Sbarba P, Lulli M. Imatinib-mesylate enhances the maintenance of chronic myeloid leukemia stem cell potential in the absence of glucose. *Stem Cell Res*. 2018;28:33–8.
24. Yao C-H, Fowle-Grider R, Mahieu NG, Liu G-Y, Chen Y-J, Wang R, et al. Exogenous fatty acids are the preferred source of membrane lipids in proliferating fibroblasts. *Cell Chem Biol*. 2016;23:483–93.
25. Qie S, Liang D, Yin C, Gu W, Meng M, Wang C, et al. Glutamine depletion and glucose depletion trigger growth inhibition via distinctive gene expression reprogramming. *Cell Cycle*. 2012;11:3679–90.
26. Mookerjee SA, Goncalves RLS, Gerencser AA, Nicholls DG, Brand MD. The contributions of respiration and glycolysis to extracellular acid production. *Biochim Et Biophys Acta (BBA) - Bioenergetics*. 2015;1847:171–81.
27. Landberg N, von Palffy S, Askmyr M, Lilljebjörn H, Sandén C, Rissler M, et al. CD36 defines primitive chronic myeloid leukemia cells less responsive to imatinib but vulnerable to antibody-based therapeutic targeting. *Haematologica*. 2018;103:447–55.
28. Drury J, Rychahou PG, He D, Jafari N, Wang C, Lee EY, et al. Inhibition of fatty acid synthase upregulates expression of CD36 to sustain proliferation of colorectal cancer cells. *Front Oncol*. 2020;10:1185.
29. Boyd AL, Reid JC, Salci KR, Aslostovar L, Benoit YD, Shapovalova Z, et al. Acute myeloid leukaemia disrupts endogenous myelo-erythropoiesis by compromising the adipocyte bone marrow niche. *Nat Cell Biol*. 2017;19:1336–47.

30. Lee P, Chandel NS, Simon MC. Cellular adaptation to hypoxia through hypoxia inducible factors and beyond. *Nat Rev Mol Cell Biol.* 2020;21:268–83.
31. Murugan AK, mTOR. Role in cancer, metastasis and drug resistance. *Sem Cancer Biol.* 2019;59:92–111.
32. Pike Winer LS, Wu M. Rapid analysis of glycolytic and oxidative substrate flux of cancer cells in a microplate. Sobol RW, editor. *PLoS ONE.* 2014;9:e109916.
33. Hashemi HF, Goodman JM. The life cycle of lipid droplets. *Curr Opin Cell Biol.* 2015;33:119–24.
34. Fuhrmann DC, Olesch C, Kurrle N, Schnütgen F, Zukunft S, Fleming I, et al. Chronic hypoxia enhances β -oxidation-dependent electron transport via electron transferring flavoproteins. *Cells.* 2019;8:172.
35. Lemberger L, Wagner R, Heller G, Pils D, Grunt TW. Pharmacological inhibition of lipid import and transport proteins in ovarian cancer. *Cancers (Basel).* 2022;14:6004.
36. Guerrero-Rodríguez SL, Mata-Cruz C, Pérez-Tapia SM, Velasco-Velázquez MA. Role of CD36 in cancer progression, stemness, and targeting. *Front Cell Dev Biol.* 2022;10:1079076.
37. Rhodes J, York RD, Tara D, Tajinda K, Druker BJ. CrkL functions as a nuclear adaptor and transcriptional activator in Bcr-Abl-expressing cells. *Exp Hematol.* 2000;28:305–10.
38. Mostazo MGC, Kurrle N, Casado M, Fuhrmann D, Alshamleh I, Häupl B, et al. Metabolic plasticity is an essential requirement of acquired tyrosine kinase inhibitor resistance in chronic myeloid leukemia. *Cancers (Basel).* 2020;12:3443.
39. Boren J, Cascante M, Marin S, Comin-Anduix B, Centelles JJ, Lim S, et al. Gleevec (STI571) influences metabolic enzyme activities and glucose carbon flow toward nucleic acid and fatty acid synthesis in myeloid tumor cells. *J Biol Chem.* 2001;276:37747–53.
40. Gottschalk S, Anderson N, Hainz C, Eckhardt SG, Serkova NJ. Imatinib (STI571)-mediated changes in glucose metabolism in human leukemia BCR-ABL-positive cells. *Clin Cancer Res.* 2004;10:6661–8.
41. Breccia M, Alimena G. The metabolic consequences of imatinib mesylate: changes on glucose, lipidic and bone metabolism. *Leuk Res.* 2009;33:871–5.
42. Salaverry LS, Lombardo T, Cabral-Lorenzo MC, Gil-Folgar ML, Rey-Roldán EB, Kornblihtt LI, et al. Metabolic plasticity in blast crisis-chronic myeloid leukemia cells under hypoxia reduces the cytotoxic potency of drugs targeting mitochondria. *Discov Onc.* 2022;13:60.
43. Cuminetti V, Arranz L. Bone marrow adipocytes: the enigmatic components of the hematopoietic stem cell niche. *JCM.* 2019;8:707.
44. Grandl G, Wolfrum C. Adipocytes at the core of bone function. *Cell Stem Cell.* 2017;20:739–40.
45. Shafat MS, Oellerich T, Mohr S, Robinson SD, Edwards DR, Marlein CR, et al. Leukemic blasts program bone marrow adipocytes to generate a protumoral microenvironment. *Blood.* 2017;129:1320–32.
46. Ye H, Adane B, Khan N, Sullivan T, Minhajuddin M, Gasparetto M, et al. Leukemic stem cells evade chemotherapy by metabolic adaptation to an adipose tissue niche. *Cell Stem Cell.* 2016;19:23–37.
47. Gonzalez MA, Olivas IM, Bencomo-Alvarez AE, Rubio AJ, Barreto-Vargas C, Lopez JL, et al. Loss of G0/G1 switch gene 2 (G0S2) promotes disease progression and drug resistance in chronic myeloid leukaemia (CML) by disrupting glycerophospholipid metabolism. *Clin Translational Med.* 2022;12:e1146.
48. Naka K. Role of lysophospholipid metabolism in chronic myelogenous leukemia stem cells. *Cancers.* 2021;13:3434.
49. Ricciardi MR, Mirabilii S, Allegretti M, Licchetta R, Calarco A, Torrisi MR, et al. Targeting the leukemia cell metabolism by the CPT1a inhibition: functional preclinical effects in leukemias. *Blood.* 2015;126:1925–9.
50. Minhajuddin M, Winters A, Ye H, Pei S, Stevens B, Gillen A et al. Lysosomal acid lipase A modulates leukemia stem cell response to venetoclax/tyrosine kinase inhibitor combination therapy in blast phase chronic myeloid leukemia. *haematol.* 2024 [cited 2025 Mar 24]; Available from: <https://haematology.ca.org/article/view/haematol.2023.284716>
51. Shinohara H, Taniguchi K, Kumazaki M, Yamada N, Ito Y, Otsuki Y, et al. Anti-cancer fatty-acid derivative induces autophagic cell death through modulation of PKM isoform expression profile mediated by bcr-abl in chronic myeloid leukemia. *Cancer Lett.* 2015;360:28–38.

Publisher's note

Springer Nature remains neutral with regard to jurisdictional claims in published maps and institutional affiliations.